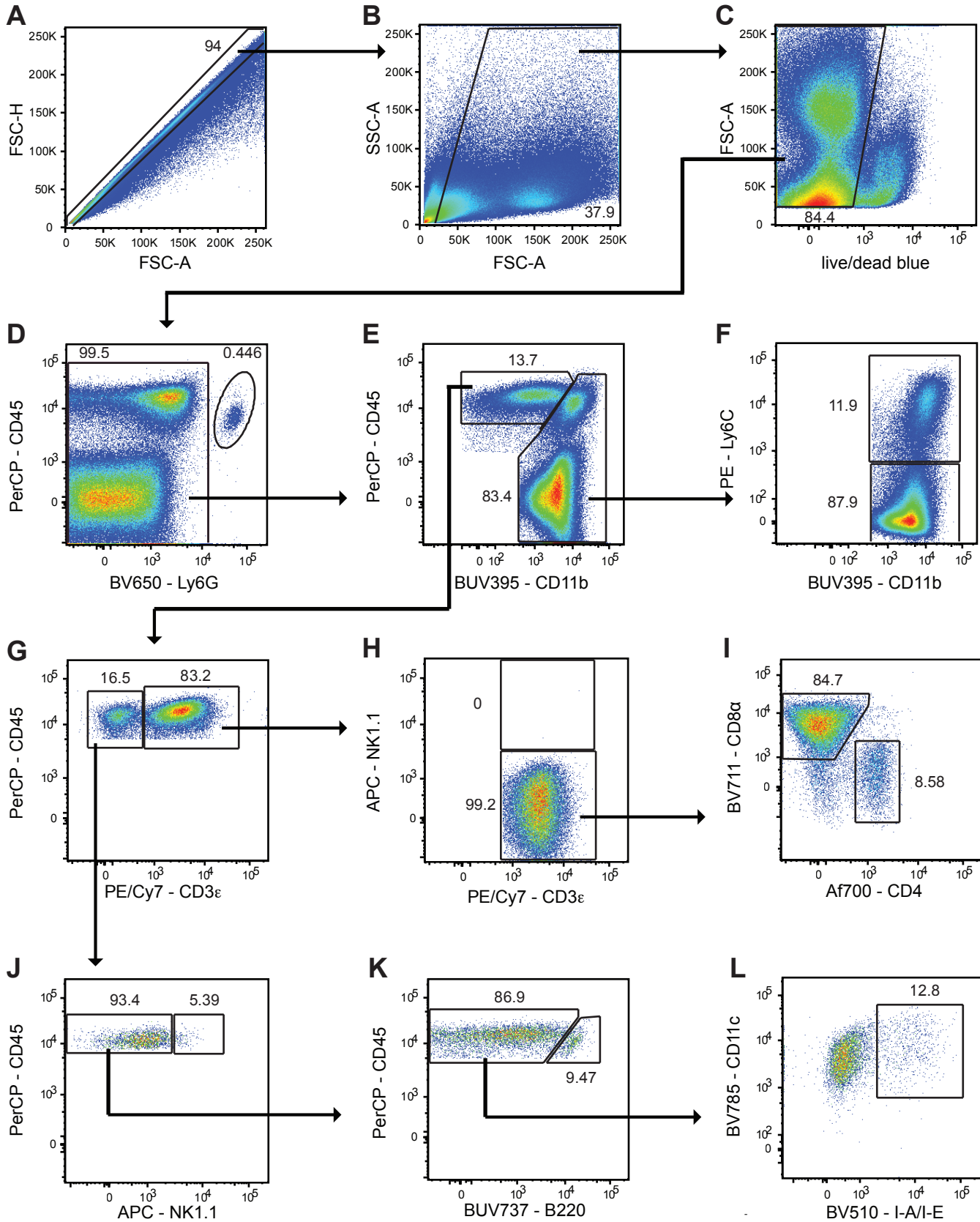


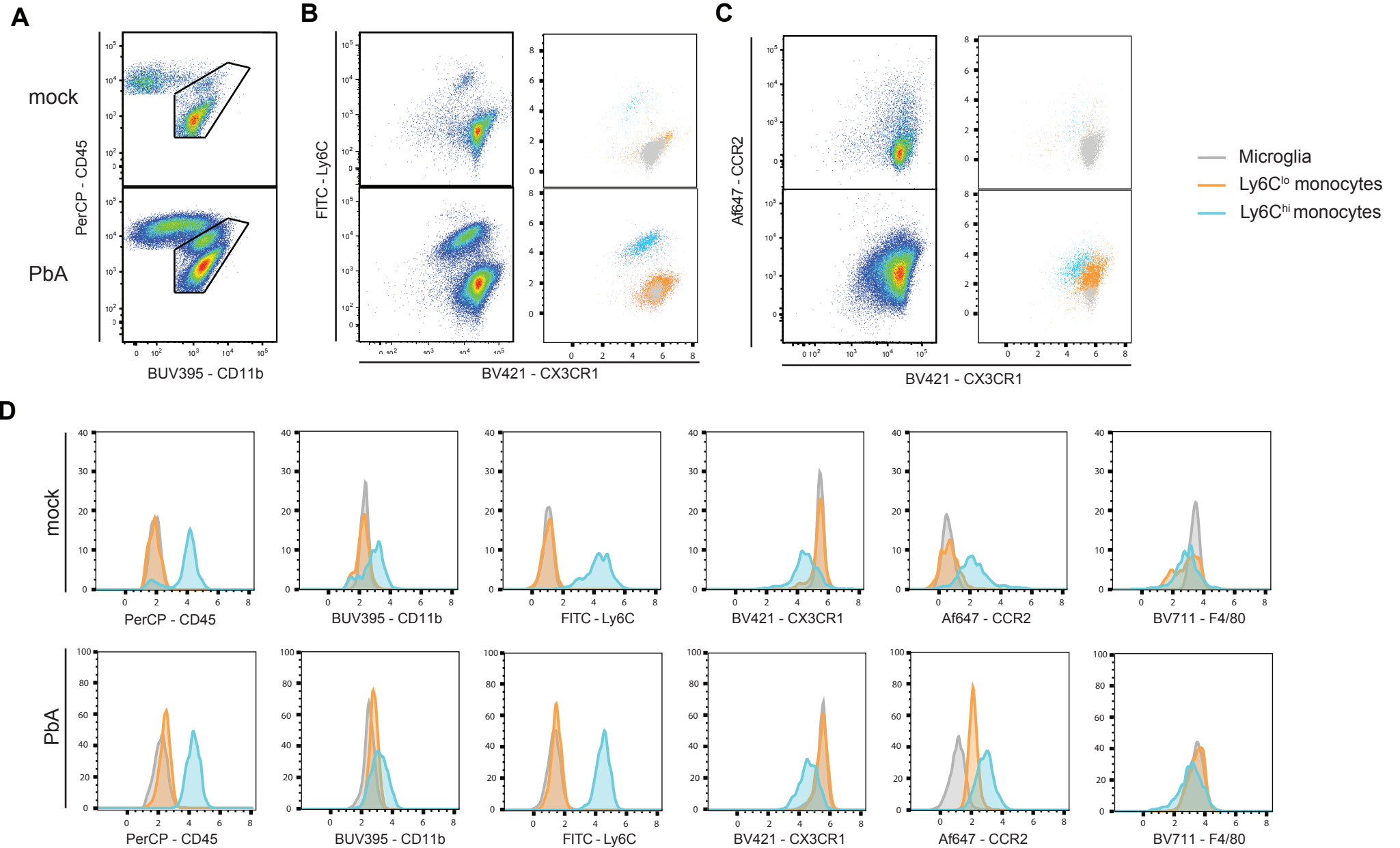
## Supplementary figure 1



### Supplementary Figure 1. Gating strategy for brain populations

Representative sequential flow cytometric gating used to identify cell populations in the PbA-infected brain on d8 p.i. Doublets (**A**), debris (**B**) and dead cells (**C**) were excluded. Neutrophils were gated as Ly6G<sup>+</sup> CD45<sup>+</sup> cells (**D**) and the remaining population was further divided into CD11b<sup>+</sup> myeloid and CD45<sup>hi</sup> lymphocytes (**E**). Myeloid cells were split into Ly6C<sup>lo</sup> and Ly6C<sup>hi</sup> cells (**F**). CD3 $\epsilon$ <sup>+</sup> cells (**G**) were split into CD3 $\epsilon$ <sup>+</sup> NK1.1<sup>+</sup> NKT cells and CD3 $\epsilon$ <sup>+</sup> NK1.1<sup>-</sup> T cells (**H**). T cells were further characterised as CD4<sup>+</sup> or CD8<sup>+</sup> T cells (**I**). CD3 $\epsilon$ <sup>-</sup> cells were identified as NK1.1<sup>+</sup> NK cells (**J**), B220<sup>+</sup> B cells (**K**) and CD11c<sup>+</sup> MHC-II<sup>+</sup> classical DC (**L**).

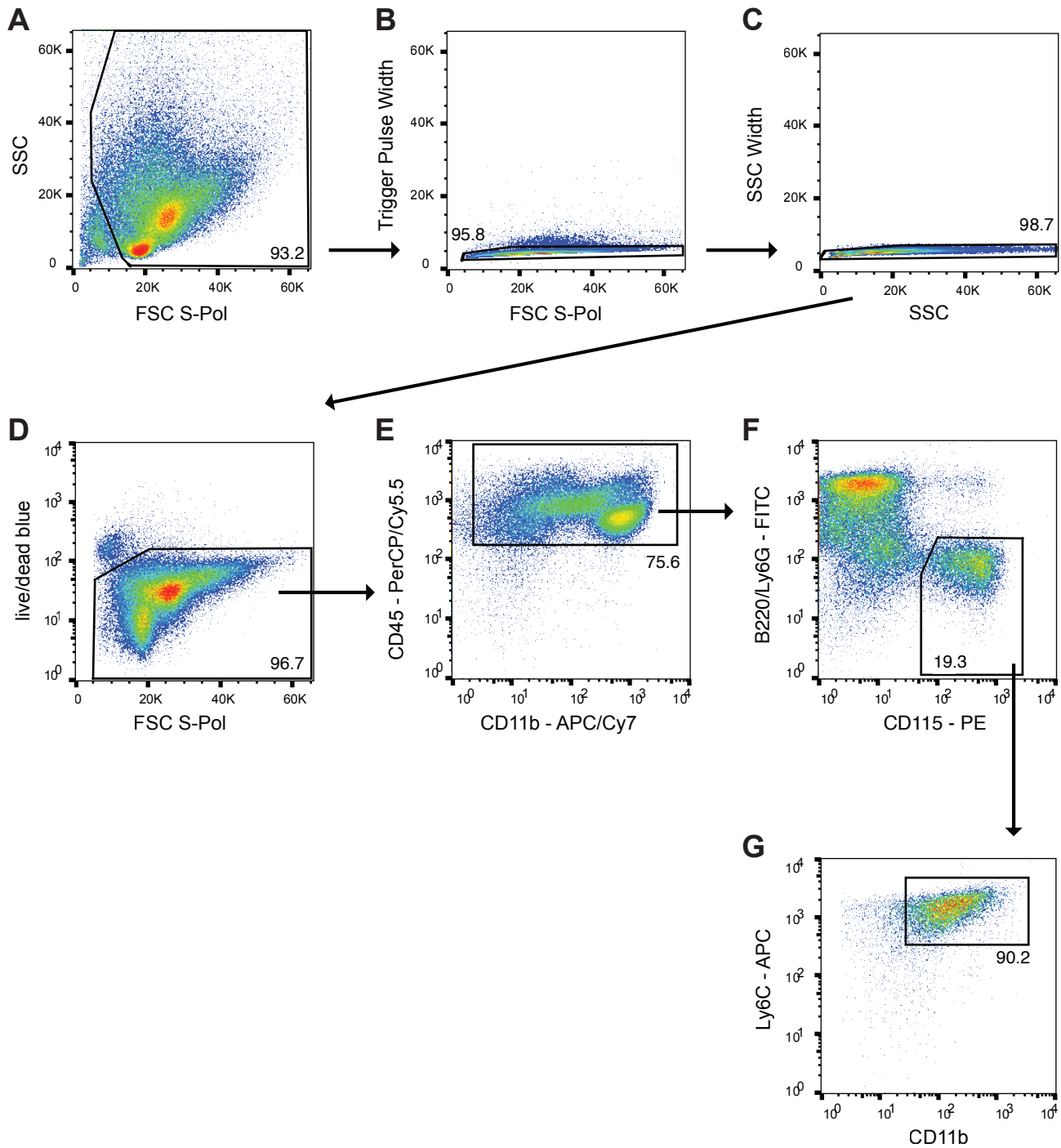
## Supplementary figure 2



### Supplementary figure 2. Detailed analysis of CD11b<sup>+</sup> brain population

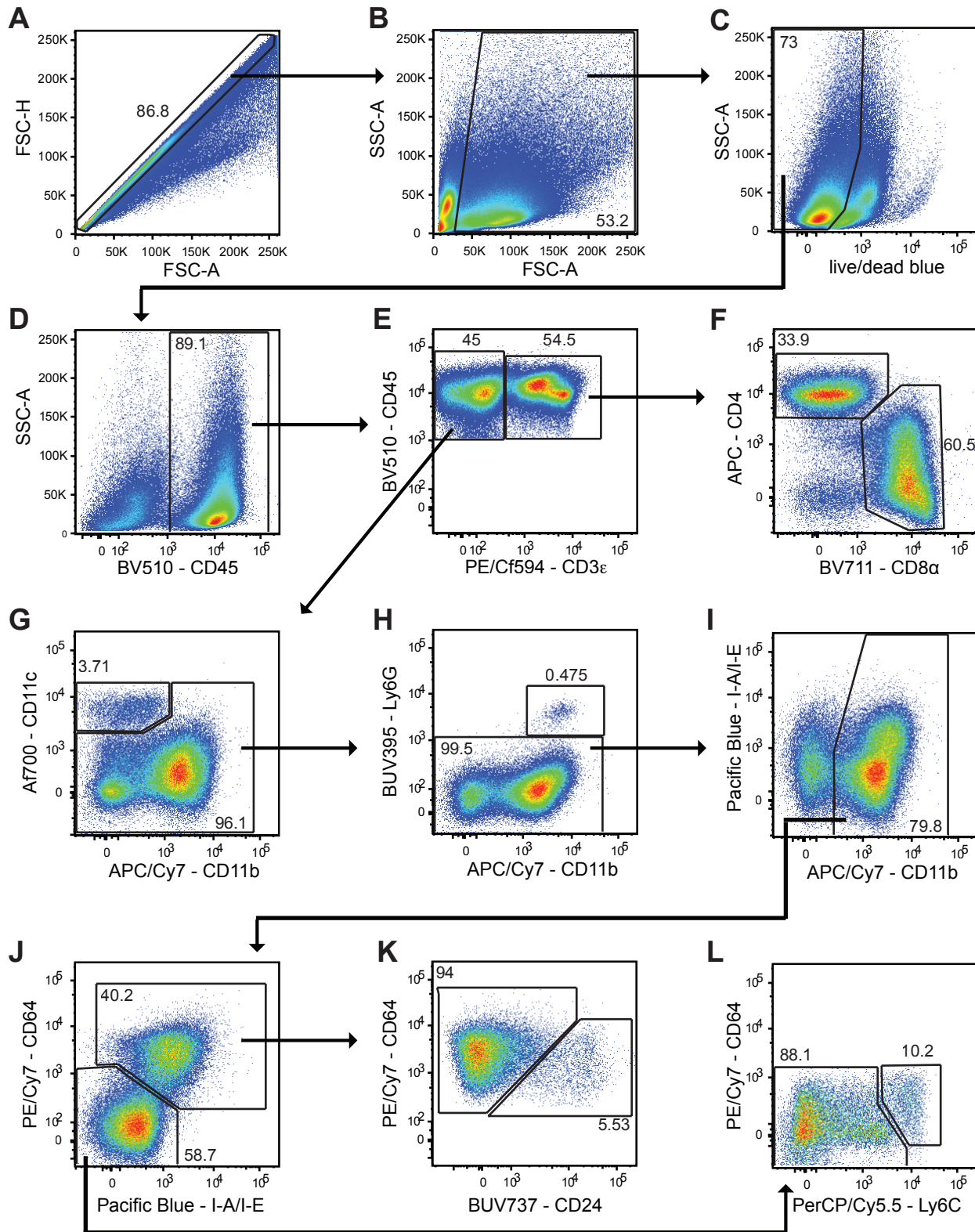
**A** Gating of the CD11b<sup>+</sup> population in the brain of mock- and d8 p.i. PbA-infected mice. **B-C** Dot plots of the CD11b<sup>+</sup> population plotted as Ly6C vs CX3CR1 (**B**) and CCR2 vs CX3CR1 (**C**) by manual analysis in FlowJo (left panels) and by overlaying the three populations from tSNE analysis onto the same plot (right panels). **D** Representative histograms showing expression of markers on the three myeloid populations resolved by tSNE in the brains of mock- and PbA-infected mice.

### Supplementary figure 3



**Supplementary figure 3. Gating strategy for sorting Ly6C<sup>hi</sup> monocytes from bone marrow isolates**  
Representative sequential flow cytometric gating used to sort Ly6C<sup>hi</sup> monocytes from the bone marrow. Exclusion of debris (A), doublets (B and C) and dead cells (D) was applied. Subsequently CD45<sup>+</sup> leukocytes were gated (E) and B220-Ly6G-CD115<sup>+</sup> monocytes (F) were selected. Of these, CD11b<sup>+</sup> monocytes with high expression of Ly6C were sorted (G).

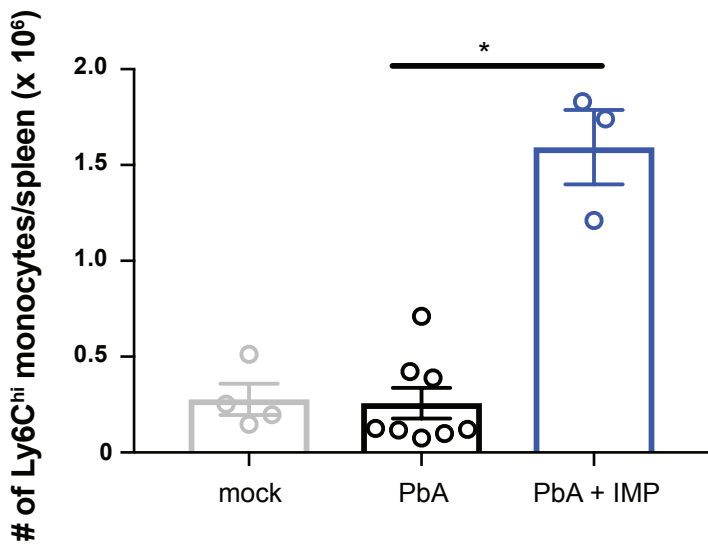
## Supplementary figure 4



### Supplementary figure 4. Gating strategy of the lung

Representative sequential flow cytometric gating used to identify cell populations in the PbA-infected lung on d8 p.i. Doublets (A), debris (B) and dead cells (C) were excluded. CD45 expression was used to gate the total leukocyte population (D). T cells were identified as CD3 $\epsilon$ <sup>+</sup> (E) and further characterised as CD4<sup>+</sup> or CD8<sup>+</sup> (F). In the CD3 $\epsilon$ <sup>+</sup> population, alveolar macrophages were identified as CD11c<sup>+</sup> CD11b<sup>lo</sup> (G). Neutrophils were gated as CD11b<sup>+</sup> Ly6G<sup>+</sup> (H). The remaining CD11b<sup>+</sup> population (I) was split into CD64<sup>-</sup> MHC-II<sup>-</sup> cells and CD64<sup>+</sup>/MHC-II<sup>+</sup> (J). Subsequently, CD64 and CD24 expression of CD64<sup>+</sup>/MHC-II<sup>+</sup> cells was used to identify CD24<sup>-</sup> interstitial macrophages and CD24<sup>+</sup> CD11b<sup>+</sup> DC (K). CD64<sup>-</sup> MHC-II<sup>-</sup> cells were divided into Ly6C<sup>lo</sup> and Ly6C<sup>hi</sup> monocytes (L).

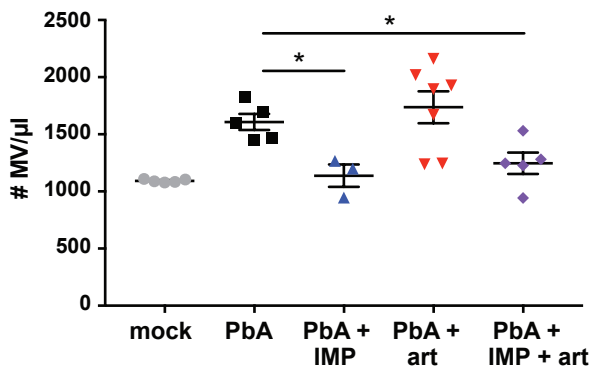
## Supplementary figure 5



### Supplementary figure 5. Ly6C<sup>hi</sup> monocytes accumulate in the spleen of IMP-treated mice

The number of Ly6C<sup>hi</sup> monocytes in the spleen of mock-infected, PbA-infected and PbA-infected, IMP-treated mice on d8 p.i. Data represents 1 experiment with a total n of 3-8 mice per group, shown as mean  $\pm$  SEM and analysed using a Kruskal-Wallis test with a Dunn's multiple comparison test.

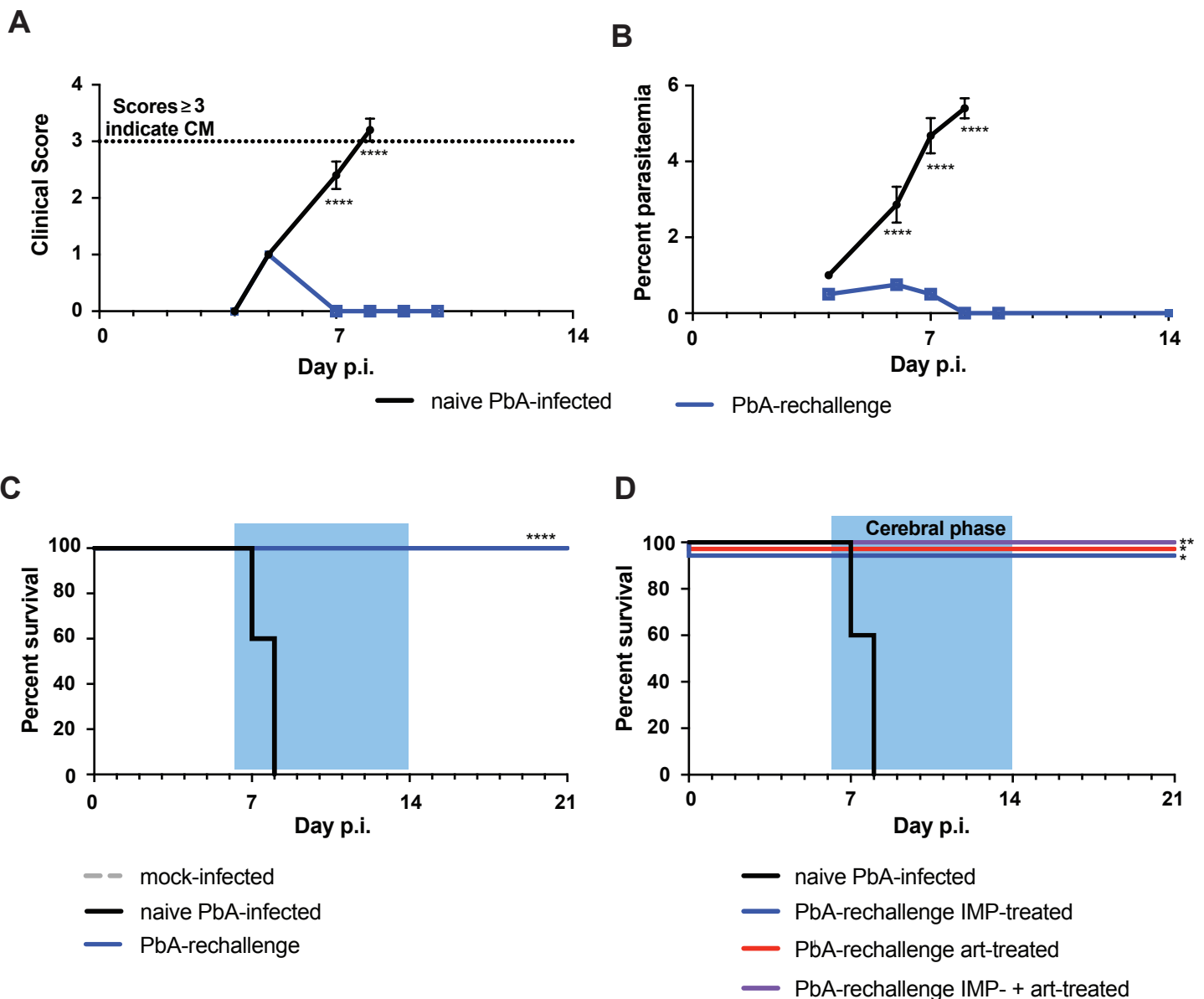
## Supplementary Figure 6



### Supplementary figure 6. Effect of treatment on circulating microvesicles

Number of circulating microvesicles per microlitre of platelet-free plasma in mock-infected mice, and in PbA-infected mice, comparing IMP, artesunate or combination treatment from d7 p.i. with untreated controls. Data represents 1 experiment with a total n of 3-7 mice per group shown as mean  $\pm$  SEM and were analysed using a Mann-Whitney test.

## Supplementary Figure 7



### Supplementary figure 7. Treated PbA-infected mice are protected during reinfection

**A-B** Clinical scores (**A**) and parasitaemia (**B**) in previously successfully treated mice, reinfected on d35 p.i., compared to naïve PbA-infected mice. **C** Survival of mice reinfected with PbA, following previous successful early IMP treatment, compared with untreated controls. The acute phase of mortality, observed during the second week post-PbA-infection, is denoted by the blue box. **D** Survival of mice reinfected with PbA, following previous successful late IMP, artesunate or combination treatment, compared with untreated controls. All rechallenged groups had 100% survival, but the lines have been separated for clarity. The acute phase of mortality, observed during the second week post-PbA-infection, is denoted by the blue box. Data in figures A-C represents 3 separate experiments with a total n of 5-16 mice per group and data in figure D represents 2 separate experiments with a total n of 3-6 mice per group. Data in figures A-B are shown as mean  $\pm$  SEM and analysed using a Kruskal-Wallis test with a Dunn's multiple comparison test comparing all groups at each timepoint. Data in figure C and D were compared using the Mantel-Cox log-rank test.

		Microglia	Ly6C <sup>lo</sup> monocytes	Ly6C <sup>hi</sup> monocytes
CD45	mock	2.032 ± 0.015	2.815 ± 0.034	3.848 ± 0.115
	PbA	2.050 ± 0.055	2.775 ± 0.076	4.463 ± 0.090
Ly6C	mock	1.320 ± 0.028	1.718 ± 0.057	3.993 ± 0.051
	PbA	1.243 ± 0.034	1.628 ± 0.062	4.348 ± 0.045
F4/80	mock	3.328 ± 0.050	4.043 ± 0.061	2.753 ± 0.107
	PbA	2.848 ± 0.200	3.518 ± 0.105	3.053 ± 0.230
CD80	mock	1.678 ± 0.009	2.355 ± 0.069	1.563 ± 0.123
	PbA	1.595 ± 0.033	2.510 ± 0.082	3.058 ± 0.288
MHC-II	mock	2.923 ± 0.048	4.018 ± 0.075	3.663 ± 0.135
	PbA	3.080 ± 0.042	3.920 ± 0.042	4.648 ± 0.220
CX3CR1	mock	5.480 ± 0.064	5.553 ± 0.094	4.495 ± 0.103
	PbA	5.043 ± 0.202	5.483 ± 0.074	4.448 ± 0.122
CD86	mock	1.005 ± 0.006	1.180 ± 0.018	1.045 ± 0.013
	PbA	1.005 ± 0.006	1.088 ± 0.017	1.068 ± 0.013
CCR2	mock	1.080 ± 0.021	2.480 ± 0.076	2.076 ± 0.015
	PbA	1.278 ± 0.050	2.505 ± 0.095	2.960 ± 0.158

**Supplementary table 1. MFI of brain populations in tSNE analysis**

MFI of indicated markers on populations in the brain of mock- and PbA-infected mice on d8 p.i., as determined by tSNE analysis. Fluorescent markers are scaled during tSNE analysis and range from 0-6.



		<b>Alveolar macrophages</b>	<b>Interstitial macrophages</b>	<b>Ly6C<sup>lo</sup> monocytes</b>
<b>CCR2</b>	mock	3.477 ± 0.055	3.737 ± 0.006	2.590 ± 0.044
	PbA	4.565 ± 0.304	4.965 ± 0.007	2.800 ± 0.057
<b>CD86</b>	mock	2.817 ± 0.055	2.683 ± 0.108	2.300 ± 0.010
	PbA	2.970 ± 0.001	2.745 ± 0.021	2.240 ± 0.001
<b>CD11b</b>	mock	3.433 ± 0.035	6.000 ± 0.096	5.877 ± 0.081
	PbA	4.220 ± 0.2545	6.000 ± 0.064	5.355 ± 0.163
<b>CX3CR1</b>	mock	3.767 ± 0.032	4.533 ± 0.091	2.853 ± 0.072
	PbA	4.330 ± 0.3677	4.770 ± 0.014	3.370 ± 0.255
<b>MHC-II</b>	mock	5.350 ± 0.030	5.720 ± 0.125	3.170 ± 0.060
	PbA	5.000 ± 0.056	5.635 ± 0.106	2.665 ± 0.049
<b>CD80</b>	mock	4.766 ± 0.091	2.49 ± 0.1769	1.191 ± 0.099
	PbA	3.750 ± 0.665	4.125 ± 0.007	1.905 ± 0.050
<b>CD206</b>	mock	5.086 ± 0.070	3.080 ± 0.265	1.923 ± 0.006
	PbA	2.820 ± 0.679	1.650 ± 0.184	2.070 ± 0.042
<b>Ly6C</b>	mock	4.573 ± 0.035	4.240 ± 0.261	3.110 ± 0.115
	PbA	4.235 ± 0.304	5.945 ± 0.007	3.060 ± 0.071
<b>CD64</b>	mock	5.333 ± 0.049	4.733 ± 0.072	2.327 ± 0.023
	PbA	5.120 ± 0.537	5.650 ± 0.226	2.385 ± 0.064

**Supplementary table 2. MFI of lung populations in tSNE analysis**

MFI of indicated markers on populations in the lung of mock- and PbA-infected mice on d8 p.i., as determined by tSNE analysis. Fluorescent markers are scaled during tSNE analysis and range from 0-6.